British Journal of Pharmacology

British Journal of Pharmacology (2016) **173** 1058–1069 1058

RESEARCH PAPER

α_{1B}-Adrenoceptor signalling regulates bone formation through the up-regulation of CCAAT/enhancer-binding protein δ expression in osteoblasts

Correspondence Takao Hirai, Department of Pharmacology, School of Dentistry, Aichi Gakuin University, 1-100 Kusumoto-cho, Chikusa-ku, Nagoya 464-8650, Japan. E-mail: t-hirai@dpc.agu.ac.jp

Received 23 April 2015; **Revised** 17 December 2015; **Accepted** 21 December 2015

Kenjiro Tanaka, Takao Hirai, Daisuke Kodama, Hisataka Kondo, Kazunori Hamamura and Akifumi Togari

Department of Pharmacology, School of Dentistry, Aichi Gakuin University, Nagoya 464-8650, Japan

BACKGROUND AND PURPOSE

The sympathetic nervous system regulates bone remodelling, in part, through ß$_2$-adrenoceptor signalling. However, the physiological role of α_1-adrenoceptor signalling in bone *in vivo* remains unclear. Therefore, to obtain a deeper understanding of bone remodelling by the sympathetic nervous system, we investigated the role of α_{1B}-adrenoceptor signalling in bone metabolism.

EXPERIMENTAL APPROACH

Prazosin, a nonspecific α_1-adrenoceptor antagonist, was administered for 2 weeks in C57BL6 mice, and efficacy was evaluated by bone microarchitecture using microcomputed tomography and determination of bone formation by fluorescent labelling of bone. We also compared the bone phenotype of α_{1B}-adrenoceptor null mice ($\alpha_{1B}^{-/-}$) with that of wild-type littermates.

KEY RESULTS

We demonstrated that the systemic administration of prazosin decreased bone formation. In addition, α_{1B}-adrenoceptor-deficient mice had a lower bone mass due to decreased bone formation but did not exhibit any changes in bone-resorbing activity. Furthermore, stimulation with phenylephrine, a non-specific α_1-adrenoceptor agonist, increased the expression of the transcriptional factor *CCAAT/enhancer-binding protein δ* (*Cebpd*) in MC3T3-E1 osteoblastic cells. The overexpression of Cebpd induced cellular proliferation in MC3T3-E1 cells, whereas the silencing of Cebpd suppressed it.

CONCLUSIONS AND IMPLICATIONS

Taken together, these results suggested that α_{1B}-adrenoceptor signalling is required for bone formation and regulated cellular proliferation through a mechanism relevant to the up-regulation of *Cebpd* in osteoblasts and, thus, provide new evidence for the physiological importance of α_{1B}-adrenoceptor signalling in bone homeostasis.

Abbreviations

BFR, bone formation rate; BMSC, bone marrow stromal cells; BV/TV, bone volume per total volume; Cebpd, CCAAT/enhancer-binding protein δ; Ctsk, cathepsin K; MAR, bone mineral apposition rate; MS/BS, mineral surface per bone surface; Nfatc1, nuclear factor of activated T-cells, cytoplasmic-1; Ob.N/BS, osteoblast number per bone surface; OC, osteocalcin; Oc.N/BS, osteoclast number per bone surface; Oc.S/BS, osteoclast surface per bone surface; Osx, osterix; RANKL, receptor activator of nuclear factor-kB ligand; Runx2, runt-related transcription factor 2; Tb.N, trabecular number; Tb.Sp, trabecular separation; Tb.Th, trabecular thickness; TRAP, tartrate-resistant acid phosphatase; WT, wild type; μCT, μ-computed tomography

DOI:10.1111/bph.13418

Tables of Links

TARGETS	
GPCRs[a]	**Catalytic receptors**[b]
α1A-adrenoceptor	Osteoprotegerin (OPG)
α1B-adrenoceptor	**Enzymes**[c]
α1D-adrenoceptor	Cathepsin K
ß2-adrenoceptor	

LIGANDS	
Noradrenaline	Prazosin
Phenylephrine	RANKL

These Tables list key protein targets and ligands in this article which are hyperlinked to corresponding entries in http://www.guidetopharmacology.org, the common portal for data from the IUPHAR/BPS Guide to PHARMACOLOGY (Pawson *et al.*, 2014) and are permanently archived in the Concise Guide to PHARMACOLOGY 2015/16 ([a,b,c]Alexander *et al.*, 2015a,b,c).

Introduction

Throughout life, bone homeostasis is maintained by remodelling and balancing osteoclast-mediated bone resorption and osteoblast-mediated bone formation. Under normal conditions bone remodelling is regulated by systemic hormones and paracrine/autocrine factors. Recent studies have demonstrated that the sympathetic nervous system plays a role in bone metabolism (Takeda *et al.*, 2002; Elefteriou *et al.*, 2005; Togari *et al.*, 2005). The actions of noradrenaline (NA) are known to be mediated through interactions with the membrane-bound adrenoceptor, which has been categorized into three families: α_1, α_2 and ß, with at least nine subtypes being identified to date: α_{1A}-, α_{1B}-, α_{1D}-, α_{2A}-, α_{2B}-, α_{2C}-, $ß_1$-, $ß_2$- and $ß_3$-adrenoceptors (Kobilka, 2011). All adrenoceptor families belong to the GPCR superfamily. We previously reported the expression of mRNA for α_{1B}- and $ß_2$-adrenoceptors in human osteoblasts (Togari, 2002). Evidence has accumulated to show that the sympathetic nervous system regulates bone remodelling and tooth movement, in part, through $ß_2$-adrenoceptors (Takeda *et al.*, 2002; Elefteriou *et al.*, 2005; Togari *et al.*, 2005; Kondo *et al.*, 2013). Previous studies revealed that $ß_2$-adrenoceptor signalling in osteoblasts suppressed bone osteoblastgenesis and increased osteoclastogenesis, thereby enhancing bone resorption (Takeuchi *et al.*, 2001; Takeda *et al.*, 2002; Elefteriou *et al.*, 2005; Togari *et al.*, 2005). α_1-Adrenoceptors were previously shown to have an important role in regulating the functionality of osteoblasts (Suzuki *et al.*, 1998, 1999; Huang *et al.*, 2009; Hirai *et al.*, 2014a, 2015a). We also reported direct nerve-osteoblast communication *in vitro* and demonstrated that NA increased cell proliferation by suppressing K^+ channels via Gi/o-coupled α_{1B}-adrenoceptors in human osteoblasts (Obata *et al.*, 2007; Kodama & Togari, 2013); however, the physiological role of α_1-adrenoceptor signalling in bone *in vivo* remains unclear. Thus, to obtain a deeper understanding of bone remodelling by the sympathetic nervous system, we investigated the role of α_1-adrenoceptor signalling in bone metabolism.

Transcription factor CCAAT/enhancer-binding protein δ (C/EBPδ, Cebpd) is a member of the C/EBP family and plays a role in cellular functions. Six members of the C/EBP family have been characterized: α, ß, δ, γ, ε and ζ (Hanson, 1998; Yamanaka *et al.*, 1998). Although all C/EBP family members share the same DNA-binding specificity, they have highly diverse tissue-specific functions (Ramji & Foka, 2002). C/EBPs act as regulators of gene expression by either direct DNA binding or interacting with other transcriptional activators (Gutierrez *et al.*, 2002). Several studies have implicated Cebpd in the regulation of target genes of diverse biological functions that include growth arrest, apoptosis, differentiation, stem cell self-renewal and tumour suppression (O'Rourke *et al.*, 1999; Thangaraju *et al.*, 2005; Gery *et al.*, 2005; Barbaro *et al.*, 2007; Sarkar *et al.*, 2012; Balamurugan & Sterneck, 2013). In osteoblasts, Cebpd has been shown to activate the transcription of insulin-like growth factor 1, which plays a key role in skeletal growth by stimulating bone cell replication and differentiation (Umayahara *et al.*, 1999).

The findings of pharmacological studies using prazosin, an α_1-adrenoceptor antagonist, and genetic studies suggested that α_{1B}-adrenoceptor signalling regulates bone mass and cellular proliferation by regulating the expression of Cebpd in osteoblasts. The results obtained will, at least in part, elucidate the mechanism underlying the regulation of bone mass by the sympathetic nervous system.

Methods

Ethics statement

All mice were treated in accordance with the Guidelines for Animal Experiments at the School of Dentistry, Aichi Gakuin University. Animal studies are reported in compliance with the ARRIVE guidelines (Kilkenny et al., 2010; McGrath and Lilley, 2015). A total of 217 mice were used in the experiments as detailed here. Food and water were available *ad libitum*. Animals were housed together in automatically controlled conditions of temperature (23 ± 1°C) and humidity (50 ± 10%) under a 12 h light : 12 h dark cycle.

Mice

α_{1B}-Adenoceptor-deficient mice ($\alpha_{1B}^{-/-}$) were provided by CARD (Center for Animal Resources and Development, Kumamoto University). The generation of $\alpha_{1B}^{-/-}$ was as described previously (Cavalli *et al.*, 1997). The $\alpha_{1B}^{-/-}$ mice had been backcrossed onto the C57BL/6 J background for more than five generations. We used $\alpha_{1B}^{-/-}$ and their wild-type (WT) littermates. The genotypes of the offspring were screened using PCR.

Drugs and treatment

C57BL/6 J mice were originally obtained from Japan SLC, Inc. (Hamamatsu, Japan). α_1-Adrenoceptor-mediated pathways

were stimulated using phenylephrine, a nonspecific α_1-adrenoceptor agonist (Sigma-Aldrich, St. Louis, MO, USA). Prazosin, a non-specific α_1-adrenoceptor antagonist (Sigma-Aldrich), was dissolved in saline at a concentration of 10 mg·mL^{-1}. Male, eight-week-old mice were randomized by wt., assigned to groups and acclimatized to their cages for 2 weeks prior to the experiment. Mice were treated with prazosin at 1, 3, 10 and 30-μg·kg^{-1} or saline i.p. every morning for 2 weeks. Body wt. was measured weekly, and the prazosin dose adjusted accordingly. Bone tissue samples were dissected and kept at −80°C for total RNA until assayed (Hirai *et al.,* 2014b).

Bone densitometry and body composition analyses

The distal region of the right femur was subjected to a three-dimensional μ-computed tomography (μCT) analysis using an R-mCT μCT scanner (RIGAKU, Tokyo, Japan). Scanning was initiated 1.0 mm above the distal femoral growth plate, and a total of 75 consecutive 20-μm-thick sections were analysed, encompassing a length of 1.5 mm of the secondary spongiosa. The measured volume of interest in the femur was obtained by selecting the cancellous bone (separate from the cortical shaft) using contour areas that were drawn semiautomatically (Tanaka *et al.,* 2015). TRI/3D-BON (Ratoc, Tokyo, Japan) software was used to analyse the cancellous parameters: bone volume per total volume (BV/TV, %), trabecular number (Tb.N, 1 mm^{-1}), trabecular thickness (Tb.Th, μm) and trabecular separation (Tb.Sp, μm).

Bone histomorphometry

In the dynamic histomorphometric analysis, all mice were injected i.p. with calcein (10 μg g^{-1}) at 4 and 2 days before death. At the end of the experiments, the right femur of each mouse was dissected and fixed in 70% ethanol. Five-micrometre-thick sagittal sections were made as undecalcified sections. To assess the bone formation rate (BFR), metaphyseal cancellous bone in the femur was used to obtain the bone fraction in a rectangular area of 0.34 mm^2 (0.5 × 0.67 mm), with its closest and furthest edges being 0.3 and 0.8 mm distal to the growth plate respectively (Tanaka *et al.,* 2015). Regarding decalcified sections, the left tibiae of mice were dissected, fixed in 4% paraformaldehyde and then decalcified in 20% EDTA for 2 weeks. Sagittal sections (5 μm thick) were made as decalcified sections and stained with tartrate-resistant acid phosphatase (TRAP) for the osteoclast analysis. Measurements were made within an area of 0.8 mm^2 (1.0 × 0.8 mm), with its closest and furthest edges being 2.0 and 3.0 mm distal to the growth plate of the proximal ends of the tibia respectively. Osteoclast number per bone surface (Oc.N/BS) and osteoclast surface per bone surface (Oc.S/BS) were evaluated by scoring TRAP-positive multinucleated cells attached to the bone surface (Hirai *et al.,* 2015b).

Cell cultures

MC3T3-E1 cells were purchased from the RIKEN Cell Bank. MC3T3-E1 cells were cultured in α-MEM (Invitrogen, Carlsbad, CA, USA) containing 10% FBS and 1% penicillin/streptomycin at 37°C in a 5% CO_2 atmosphere. To induce differentiation, the culture medium was replaced with α-MEM containing 50 μg·mL^{-1} ascorbic acid and 5 mM ß-glycerophosphate. The culture medium was changed every 2–3 days (Hirai *et al.,* 2014a).

Construction of expression plasmids and transfection

The entire coding sequence of mouse Cebpd cDNAwas amplified by KOD-plus Neo DNA polymerase (Toyobo, Japan) and inserted into the mammalian expression vector pcDNA3. The primers used were as follows: forward 5′-CGC-GGATCCCCAACTTGGACGCCAGGTC-3′ and reverse 5′-TGCTCTAGACAGAGTCTCAAAGGCCCACG-3′. Amplified DNA was cloned into the pcDNA3 vector at the BamHI and XbaI restriction enzyme sites (underlined). The correct sequences of the subcloned cDNA fragments were confirmed by complete nucleotide sequencing (Hirai *et al.,* 2014b). MC3T3-E1 cells were plated at a density of 1.0 × 10^5 cells-cm^{-2}. Cells were transfected after 24 h with pcDNA-Cebpd, or the empty vector using FuGENE HD reagent (Promega, Madison, WI, USA) according to the manufacturer's instructions.

Generation of MC3T3-E1 cell lines with the stable expression of Cebpd

MC3T3-E1 cells were maintained in α-MEM supplemented with 10% FBS, 1% penicillin/streptomycin at 37°C in a 5% CO_2 atmosphere. Two micrograms of pcDNA3-negative and full-length Cebpd were stably transfected into MC3T3-E1 cells by FuGENE HD, followed by drug selection with 800-μg·mL^{-1} of the neomycin analogue G418. Resistant colonies were selected and expanded. Twenty stable lines (Cebpd series) were established. All subsequent experiments were conducted with three of these lines, Cebpd −1, −2 and −3, which expressed high levels of Cebpd.

siRNA nucleofection

MC3T3-E1 cells were grown in α-MEM supplemented with 10% FBS and 1% penicillin/streptomycin to ~70% confluency, followed by transient transfection with either siRNA targeting Cebpd or non-silencing RNA diluted in Opti-MEM using Lipofectamine RNAiMAX (Invitrogen) according to the manufacturer's protocol. Silencer select siRNAs were used (Ambion/Applied Biosystems, Foster City, CA, USA). Cebpd siRNAs and non-silencing RNA were both used at final concentrations of 10 nM. The medium was then replaced with fresh medium. Cells were harvested for total RNA extraction at the indicated time points.

5-Bromo-2′-deoxyuridine (BrdU) incorporation assay

Cell proliferation activity was assessed by BrdU incorporation using the Cell Proliferation ELISA BrdU kit (Roche Applied Science, Penzberg, Germany) according to the manufacturer's instructions (Kodama & Togari, 2013). MC3T3-E1 cells were grown in α-MEM supplemented with 10% FBS and 1% penicillin/streptomycin to ~70% confluency, followed by transfection with either siRNA targeting Cebpd or non-silencing RNA diluted in Opti-MEM using Lipofectamine RNAiMAX (Invitrogen) according to the manufacturer's protocol. After 6 h, culture media were replaced with fresh α-MEM containing 10% FBS. BrdU-labelling solution (100 μM) was added at 20 μL per well, and the cells were incubated for an additional 4 h at 37°C. After this, the labelling

media were removed, cells were fixed and DNAwas denatured with FixDenat solution. The cells were incubated with a peroxidase-conjugated anti-BrdU antibody for 1.5 h at room temperature. The cells were then washed three times with PBS, followed by the addition of substrate solution (tetraethyl-benzidine) at 100 μL per well. After a 15 min incubation, 1 M H_2SO_4 was added at 25 μL per well to stop the peroxidase reaction, and the absorbance of wells was measured at 450 nm using Multiskan FC (Thermo Fisher Scientific, Waltham, MA, USA).

RNA extraction and real-time PCR

Total RNA was isolated with an RNeasy Mini Kit (Qiagen, Hilden, Germany) according to the protocol of the manufacturer. One microgram of RNA was reverse transcribed into cDNA using the QuantiTect Reverse Transcription Kit according to the protocol of the manufacturer (Qiagen). Gene expression was analysed with the Step-One-Plus real-time PCR system with StepOne software v2.0 (Applied Biosystems). Reactions were performed in 20 μL volumes using a QuantiTect SYBR Green PCR Kit (Qiagen). Cycling conditions were 50°C for 2 min, 95°C for 10 min, followed by 40 cycles of 95°C for 15 s and 60°C for 1 min. The relative quantity for each sample was normalized to the average level of the constitutively expressed housekeeping gene *Gapdh*. The primers used are listed in Supporting Information Table S1. As needed, the amplified fragment by PCR was cloned and subjected to automated sequencing (Hirai *et al.,* 2009).

Data analysis

The data and statistical analysis comply with the recommendations on experimental design and analysis in pharmacology (Curtis et al., 2015). All data are expressed as mean ± SEM. The two-tailed *t*-test combined with Bonferroni's correction following one-way ANOVA was used for multiple comparisons. Differences with P values < 0.05 were considered significant.

Results

Decrease in bone mass by the systemic administration of prazosin to mice

To evaluate the functionality of α_1-adrenoceptor signalling in bone, we investigated the effects of the pharmacological blockade of α_1-adrenoceptor signalling on bone mass by performing μCT-based bone densitometry in bones after the systemic administrations of prazosin, an α_1-adrenoceptor antagonist, at 10 and 30 $\mu g \cdot kg^{-1}$ for 2 weeks. As shown in Figure 1A, the bone volume per trabecular volume (BV/TV) of the distal end of the femur of 12-week-old males was significantly lower in prazosin-treated mice at 30 $\mu g \cdot kg^{-1}$ than in saline-treated mice. No significant differences were observed in the Tb.Th or Tb.N between mice injected i.p. with prazosin in the range of 1–30 $\mu g \cdot kg^{-1}$ and saline-treated mice (Figure 1B, C). Moreover, Tb.Sp of the femur was significantly greater in prazosin-treated mice in the range of 3–30 $\mu g \cdot kg^{-1}$ than in saline-treated mice (Figure 1D). The administration

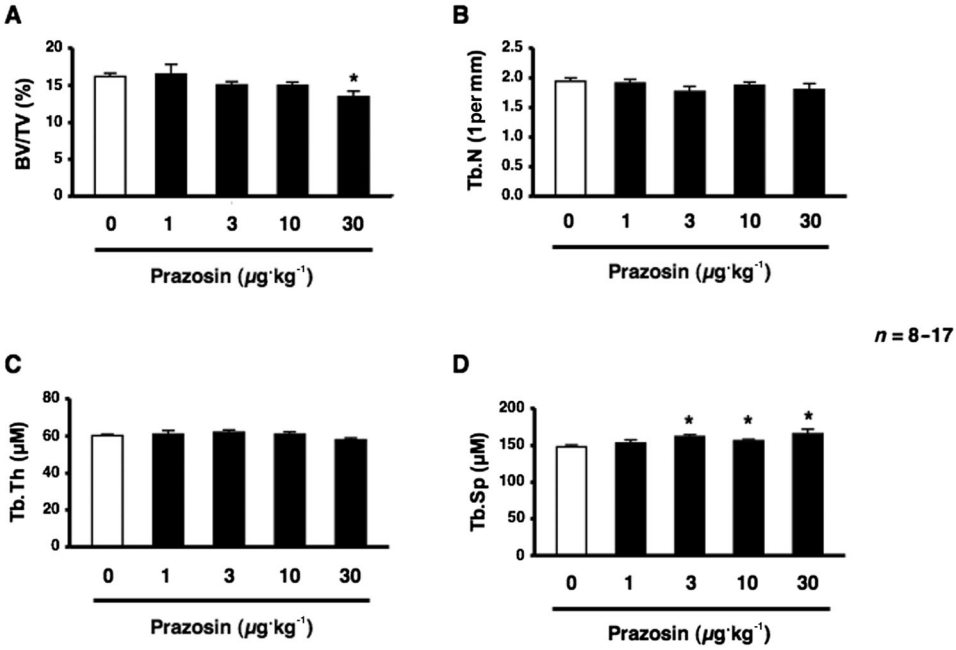

Figure 1

Blockade of α_1-adrenoceptor signalling impaired cancellous bone mass in mice. (A–D) μCT-based bone densitometry of the distal region of the femur in 12-week-old male mice administered saline (white bar) or prazosin at 1, 3, 10 and 30 $\mu g \cdot kg^{-1}$ body wt. day^{-1} for 2 weeks. (A) BV/TV. (B) Tb.N. (C) Tb.Th. (D) Tb.Sp. $n = 8$ or 17 mice per group. Similar results were obtained in three independent experiments. Values are expressed as means ± SEM. $^*P < 0.05$ significantly different from control mice.

of prazosin in the range of 1–1000 μg·kg^{-1} had no effect on body wt. These results suggest that the dose of prazosin used in this study did not have adverse effects. To examine the mechanisms responsible for bone loss due to the prazosin treatment, we performed a bone histomorphometric analysis on bone formation parameters by assessing calcein double

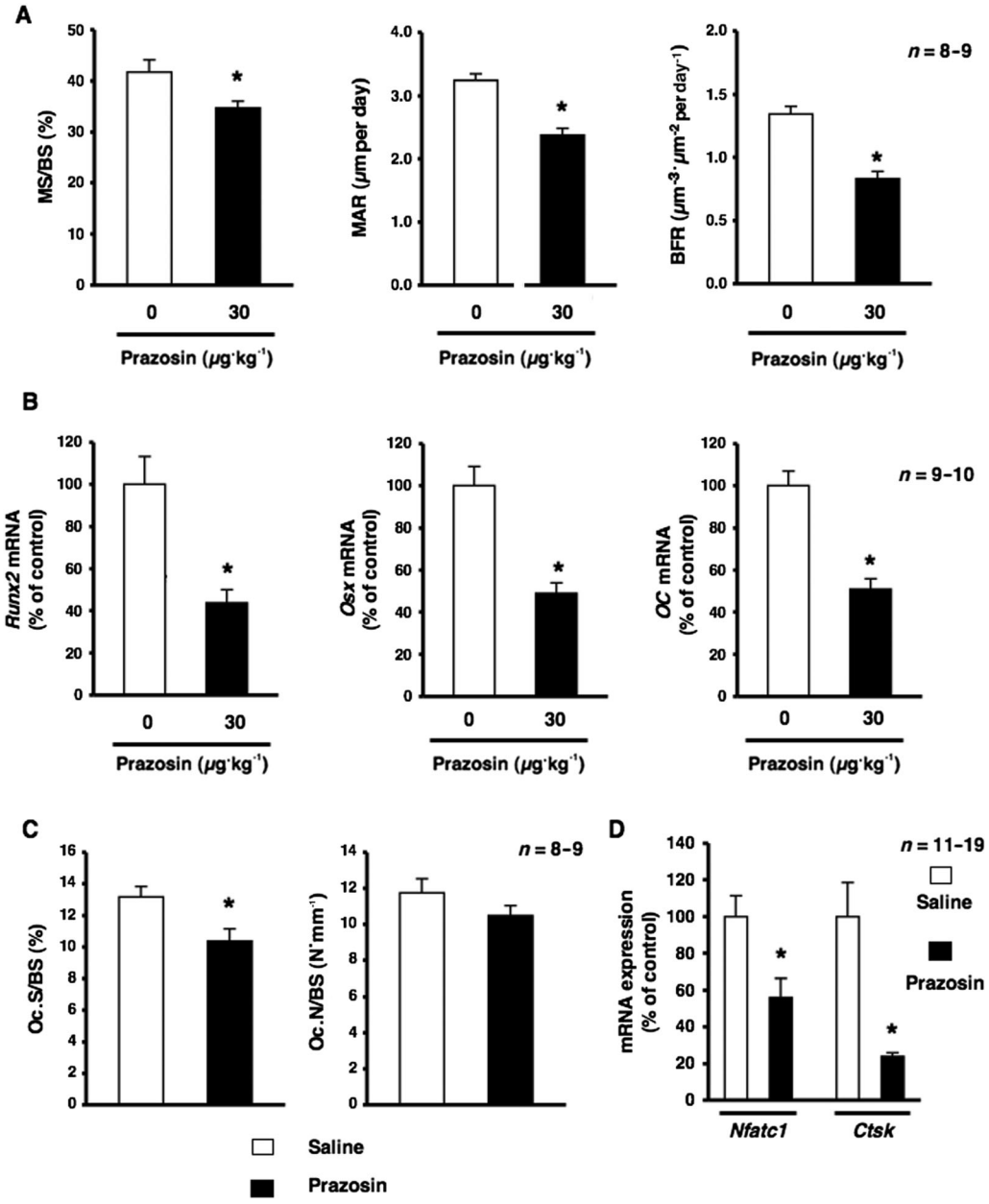

Figure 2

Effects of the systemic administration of prazosin on osteoblastic bone formation and resorption in mice. (A) An analysis of the MS/BS, MAR and BFR in the cancellous bone compartment of the distal femur metaphysis of mice administered saline and prazosin; $n = 8$ or 9 mice per group. Similar results were obtained in three independent experiments. Values are expressed as means ± SEM; $^{*}P < 0.05$, significantly different from each control value. (B) Effects of the systemic administration of prazosin on *Runx2*, *Osx* and *OC* mRNA expression in cancellous bone. Total RNA was isolated from the distal region of the femur in 12-week-old male mice administered saline or prazosin, followed by the determination of *Runx2*, *Osx* and *OC* mRNA levels by real-time qRT-PCR using specific primers; $n = 9$ or 10 mice per group. Similar results were obtained in three independent experiments. Values are expressed as means ± SEM; $^{*}P < 0.05$, significantly different from each control value. (C) Mice were treated with prazosin at 30 μg·kg^{-1} per day or saline for 2 weeks, followed by the staining of osteoclasts with TRAP. The amounts of Oc.S/BS and Oc.N/BS were measured ($n = 8$ or 9 mice per group). Values are expressed as means ± SEM. $^{*}P < 0.05$ significantly different from the control. (D) Effects of the systemic administration of prazosin on *Nfatc1* and *Ctsk* mRNA expression in bone. Total RNA was isolated from the distal region of the femur in 12-week-old male mice administered saline or prazosin, followed by the determination of *Nfatc1* and *Ctsk* mRNA levels by real-time qRT-PCR using specific primers. $n = 11$ or 19 mice per group. Values are expressed as means ± SEM. $^{*}P < 0.05$ significantly different from the control.

labelling in the distal femur after the systemic administration of prazosin for 2 weeks. This analysis provided an *in vivo* estimate of osteoblastic activity with respect to the accumulation of bone mass. Bone formation parameters such as mineral surface per bone surface (MS/BS), the bone mineral apposition rate (MAR) and BFRs were significantly lower in prazosin-treated mice than in saline-treated mice (Figure 2A). We then examined the expression of gene-related bone formation using a quantitative real-time PCR analysis. We extracted total RNA from the distal end of the femur and analysed the mRNA expression of *Runt-related transcription factor 2* (*Runx2*), *osterix* (*Osx*) and *osteocalcin* (*OC*). Consistent with the decrease observed in bone formation, the mRNA expression of *Runx2*, *Osx* and *OC* in bone was significantly decreased in prazosin-treated mice (Figure 2B), indicating that mice administered the α_1-adrenoceptor antagonist had a lower bone mass concomitant with decreased bone formation.

To confirm the effects of prazosin on bone resorption, we next performed a bone histomorphometric analysis on bone resorption parameters such as the bone surface covered by osteoclasts (Oc.S/BS) and Oc.N/BS with TRAP-positive osteoclasts. The results obtained showed that Oc.S/BS of the femur was significantly lower in prazosin-treated mice at 30 $\mu g \cdot kg^{-1}$ than in control mice. No significant differences were observed in Oc.N/BS between mice administered prazosin 30 $\mu g \cdot kg^{-1}$ i.p. and control mice (Figure 2C). In addition, the mRNA expression of osteoclast-related genes such as *cathepsin K* (*Ctsk*) and *nuclear factor of activated T-cells, cytoplasmic-1* (*Nfatc1*) was significantly decreased in prazosin-treated mice, suggesting impaired bone resorption (Figure 2D).

Ablation of α_{1B}-adrenoceptors decreased femoral cancellous bone mass

The pharmacological blockade of α_1-adrenoceptor signalling significantly decreased bone mass, as reflected by decreased bone formation, which suggested that α_1-adrenoceptor signalling, played an important role in modulating bone physiology. α_1-Adrenoceptors have been classified into three subtypes: α_{1A}, α_{1B} and α_{1D}. In order to identify the α_1-adrenoceptor subtypes expressed by osteoblasts and osteoclasts, we performed real-time PCR using primers specific for each receptor subtype. α_{1B}- and α_{1D}-adrenoceptors were expressed in MC3T3-E1 and differentiated MC3T3-E1 cells cultured in α-MEM containing 10% FBS, 50 $\mu g \cdot mL^{-1}$ ascorbic acid and 5 mM ß-GP (Supporting Information Fig. S1). In addition, we showed the expression of mRNA for the receptors of α_{1B}- and α_{1D}-adrenoceptors in bone marrow stromal cells (BMSCs) (Supporting Information Fig. S1). Therefore, to elucidate the mechanisms responsible for bone loss due to the prazosin treatment and the functional role of α_1-adrenoceptor signalling in bone metabolism, we next compared the bone phenotype of α_{1B}-adrenoceptor null mice ($\alpha_{1B}^{-/-}$) with that of WT littermates. The results of μCT-based bone densitometry showed that BV/TVof the distal end of the femurs of 10-week-old males was significantly lower in $\alpha_{1B}^{-/-}$ mice than in WT mice (Figure 3A). Moreover, the Tb.N of the femur was

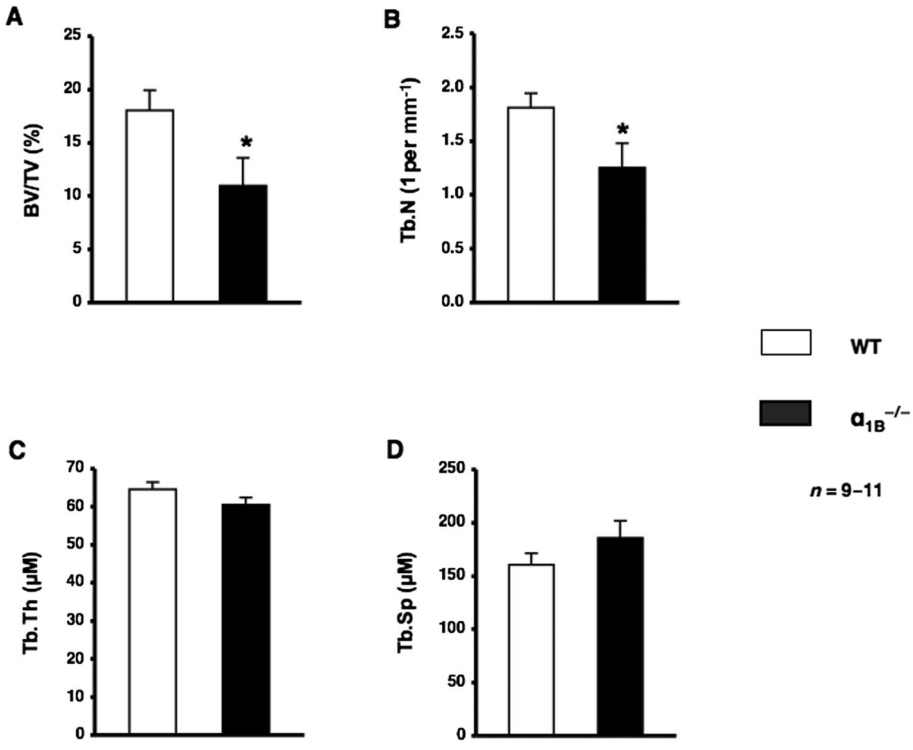

Figure 3

Ablation of α_{1B}-adrenoceptors led to a decreased bone mass. (A–D) μCT-based bone densitometry of the distal region of the right femur from WT mice and $\alpha_{1B}^{-/-}$ mice. (A) BV/TV. (B) Tb.N. (C) Tb.Th. (D) Tb.Sp. $n = 9$ or 11 mice per group. Values are expressed as means ± SEM. $^*P < 0.05$ significantly different from WT mice.

also significantly lower in $\alpha_{1B}^{-/-}$ mice than in WT mice (Figure 3B). No significant differences were observed in Tb.Th or Tb.Sp between WT and $\alpha_{1B}^{-/-}$ mice (Figure 3C, D). To elucidate further the mechanisms responsible for the α_{1B}-adrenoceptor deficiency leading to bone loss, we examined the parameters of bone formation. We observed a significant decrease in osteoblast number per bone surface (Ob.N/BS), and a reduced MS/BS, and MAR in $\alpha_{1B}^{-/-}$ mice (Figure 4A–C). BFR was also significantly decreased by approximately 40% in $\alpha_{1B}^{-/-}$ mice (Figure 4D). Furthermore, the mRNA expression of *Runx2*, *Osx* and *OC* in bone was significantly lower in $\alpha_{1B}^{-/-}$ mice than in WT littermates (Figure 4E). In contrast, no significant differences were observed in Oc.S/BS or Oc.N/BS between $\alpha_{1B}^{-/-}$ mice and WT mice (Figure 4F), indicating that their decreased bone mass was associated with a reduction in osteoblast number and activity, not changes in osteoclasts.

α_1-Adrenoceptor signalling up-regulated Cebpd gene expression in MC3T3-E1 osteoblastic cells

To investigate the physiological function of α_1-adrenoceptor signalling in osteoblasts and identify the target molecules of α_1-adrenoceptor signalling, we examined the expression of genes in response to phenylephrine in MC3T3-E1 cells. Total RNA was extracted from MC3T3-E1 osteoblastic cells exposed to phenylephrine for 1, 2, 4 and 8 h and analysed by real-time qRT-PCR. As shown in Figure 5A, the expression of *Cebpd* mRNA was significantly increased by the exposure to phenylephrine for 1 and 2 h. In addition, pretreatment with the α_1-adrenoceptor antagonist prazosin completely inhibited phenylephrine -induced *Cebpd* expression, as determined using a real-time qRT-PCR analysis in MC3T3-E1 osteoblastic cells, which suggested that the phenylephrine -induced expression of *Cebpd* was mediated by α_1-adrenoceptor signalling in MC3T3-E1 osteoblastic cells (Figure 5B). Furthermore, we investigated the effects of the pharmacological blockade of α_1-adrenoceptor signalling on the expression of *Cebpd* in cancellous bone. We extracted total RNA from the distal end of the femur and analysed the expression of *Cebpd* mRNA after the systemic administration of prazosin for 2 weeks. As shown in Figure 5C, the expression of *Cebpd* mRNA in cancellous bone was significantly lower in prazosin-treated mice than in saline-treated mice. Furthermore, we compared the expression of *Cebpd* mRNA in $\alpha_{1B}^{-/-}$ mice and WT littermates.

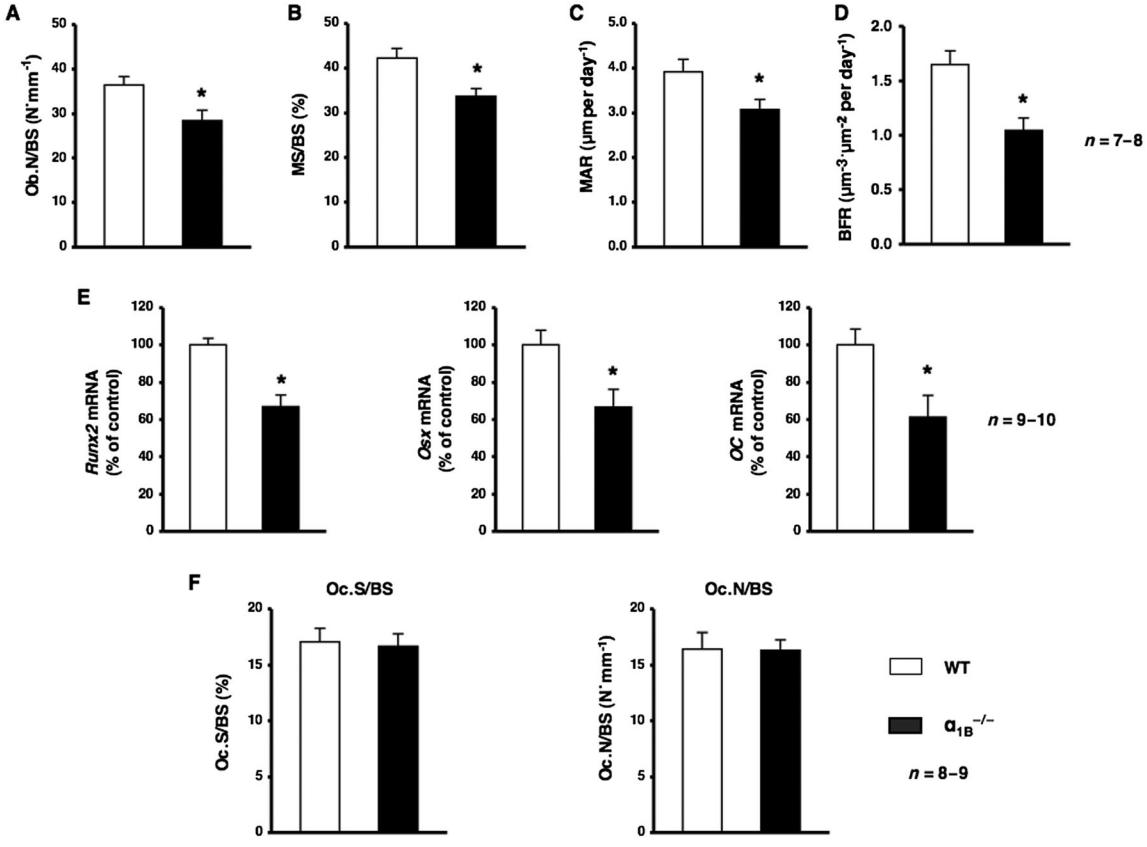

Figure 4

Ablation of α_{1B}-adrenoceptors led to a decrease in bone formation**.** (A–D) An analysis of the Ob.N/BS, MS/BS, MAR and BFR in the cancellous bone compartment of the distal femur metaphysis from WT mice and $\alpha_{1B}^{-/-}$ mice; $n = 7$ or 8 mice per group. (A) Ob.N/BS. (B) MS/BS. (C) MAR. (D) BFR. Values are expressed as means ± SEM. $^*P < 0.05$, significantly different from WT mice. (E) Total RNA was isolated from the distal region of the femur from WT and $\alpha_{1B}^{-/-}$ mice, followed by the determination of *Runx2*, *Osx* and *OC* mRNA levels by real-time qRT-PCR using specific primers; $n = 9$ or 10 mice per group. Values are expressed as means ± SEM. $^*P < 0.05$, significantly different from WT mice. (F) Sections of the primary trabecular regions of the femur from WT or α_{1B}-adrenoceptor-deficient mice followed by the staining of osteoclasts with TRAP. The amount of Oc.S/BS and Oc.N/BS were measured ($n = 8$ or 9 mice per group).

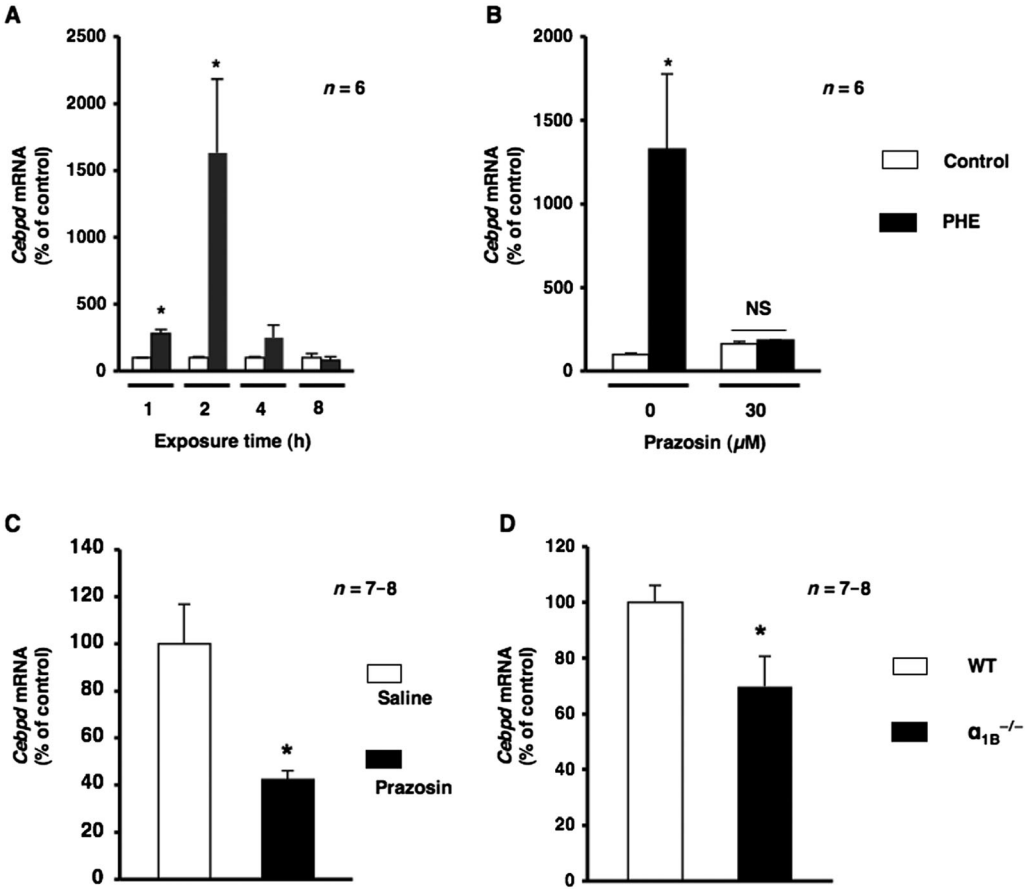

Figure 5

α_1-Adrenoceptor signalling mediated *Cebpd* expression. (A) Cells were treated with 10 μM phenylephrine (PHE) for 1, 2, 4 and 8 h, harvested and then processed for real-time qRT-PCR. Each value represents the mean ± SEM of six separate experiments. $^*P < 0.05$, significantly different from each control value obtained in MC3T3-E1 cells cultured in the absence of PHE. (B) α_1-Adrenoceptor signalling mediated *Cebpd* mRNA expression after the PHE stimulation in MC3T3-E1 cells. Cells were incubated for 2 h in the presence of PHE with prazosin at a concentration of 10 μM, followed by the determination of *Cebpd* levels by real-time qRT-PCR. Each value represents the mean ± SEM of six separate experiments. $^*P < 0.05$, significantly different from each control value. NS; not significant. (C) α_1-Adrenoceptor signalling regulated *Cebpd* in bone. Effects of the systemic administration of prazosin on *Cebpd* mRNA expression in cancellous bone. Total RNA was isolated from the distal region of the femur in 10-week-old male mice administered saline or prazosin, followed by the determination of *Cebpd* mRNA levels by real-time qRT-PCR using specific primers; $n = 7$ or 8 mice per group. Values are expressed as means ± SEM. $^*P < 0.05$, significantly different from each control value. (D) Total RNA was isolated from the distal region of the femur from WT and $\alpha_{1B}^{-/-}$ mice, followed by the determination of *Cebpd* mRNA levels by real-time qRT-PCR using specific primers. $n = 7$ or 8 mice per group. Values are expressed as means ± SEM. $^*P < 0.05$, significantly different from WT mice.

The expression of *Cebpd* mRNA in bone was significantly lower in $\alpha_{1B}^{-/-}$ mice than in WT littermates (Figure 5D), suggesting that α_{1B}-adrenoceptor signalling in osteoblasts plays a significant role in regulating *Cebpd* gene expression. Therefore, we expected Cebpd to be one of the target molecules of α_{1B}-adrenoceptor signalling in osteoblasts.

Cebpd was involved in cell proliferation in MC3T3-E1 cells

To investigate the physiological function of α_{1B}-adrenoceptor signalling in osteoblasts, we determined whether Cebpd contributed to the regulation of cellular function in osteoblasts. Based on previous findings in which α_1-adrenoceptor signalling in osteoblasts mediated cellular proliferation (Suzuki *et al.*, 1998; Kodama & Togari, 2013), we investigated whether Cebpd in osteoblasts contributed to cellular proliferation. Cebpd was silenced in MC3T3-E1 cells, and cell proliferation activity was evaluated as DNA synthesis by the BrdU incorporation assay. Cells were cultured for 24 h, transfected with *Cebpd* siRNA (or non-targeting siRNA) and then cultured for a further 24 h. As shown in Figure 6A, the incorporation of BrdU was significantly lower in these cells compared with those transfected with non-targeting control siRNA. In addition, the expression of *Ccne1*, which encodes cyclin E1, was significantly decreased in *Cebpd*-silenced cells (Figure 6B). The overexpression of Cebpd significantly increased cellular proliferation in MC3T3-E1 cells (Figure 6C). These results indicated that *Cebpd* regulated cellular proliferation in MC3T3-E1 cells. Furthermore, we observed that PHE-induced cellular proliferation was significantly decreased in MC3T3-E1 cells transfected with *Cebpd* siRNA 24 h after transfection

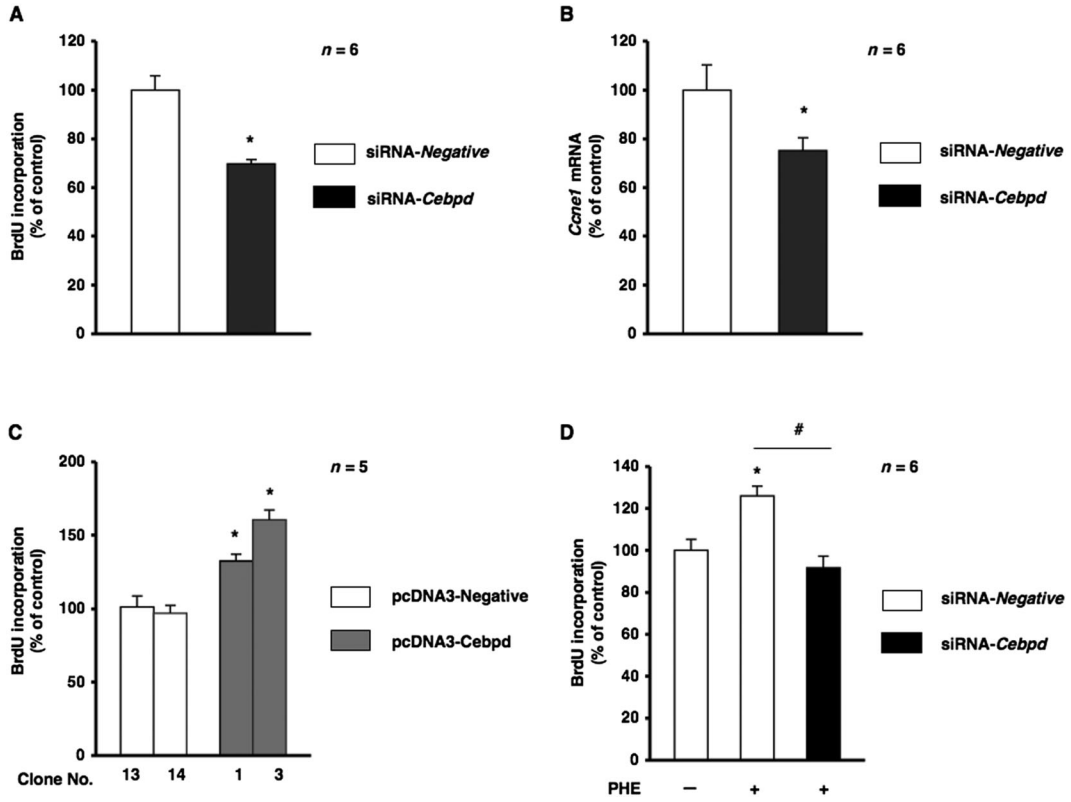

Figure 6

Cebpd was involved in cellular proliferation in MC3T3-E1 cells.(A) Effects of silencing *Cebpd* on DNA synthesis as measured by the incorporation of BrdU. MC3T3-E1 cells were treated with *Cebpd* siRNA (siRNA-*Cebpd*) or non-silencing RNA (siRNA-*Negative*), followed by the determination of BrdU incorporation according to the indicated protocols (mean ± SEM, n = 6). $^{*}P < 0.05$, significantly different from each control value. (B) MC3T3-E1 cells were treated with *Cebpd* siRNA (siRNA-*Cebpd*) or non-silencing RNA (siRNA-*Negative*) according to the indicated protocols. Real-time qRT-PCR analyses of transcription levels were performed using their specific primers for *Ccne1*. Relative mRNA expression was normalized to *Gapdh* (mean ± SEM, n = 6). $^{*}P < 0.05$, significantly different from each control value. (C) Effects of the overexpression of Cebpd in MC3T3-E1 cells. MC3T3-E1 cells were stably transfected with expression vectors for Cebpd (pcDNA-Cebpd) or control (pcDNA-Negative) followed by the determination of BrdU incorporation according to the indicated protocols (mean ± SEM, n = 5). $^{*}P < 0.05$, significantly different from the value obtained in cells transfected with the control vector. (D) Effects of *Cebpd*-knockdown by siRNA on phenylephrine (PHE)-regulated cellular proliferation in MC3T3-E1 cells. MC3T3-E1 cells were treated with *Cebpd* siRNA (siRNA-*Cebpd*) or non-silencing RNA (siRNA-*Negative*), followed by further cultivation for 24 h in the absence or presence of PHE at a concentration of 0.3 μM, and subsequent determination of BrdU incorporation (mean ± SEM, n = 6). $^{*}P < 0.05$, significantly different from value of siRNA-*Negative*. $^{\#}P < 0.05$, significantly different from the value obtained in cells treated with siRNA-*Negative* in the presence of PHE. Each figure is representative data from three independent experiments.

(Figure 6D). Taken together, these results indicate that Cebpd promotes cellular proliferation in response to α_{1B}-adrenoceptor signalling in osteoblasts.

Discussion

In the present study, we presented *in vitro* and *in vivo* evidence for the importance of α_{1B}-adrenoceptor signalling in bone homeostasis. Both the pharmacological and genetic ablation of α_{1B}-adrenoceptor signalling impaired bone mass by decreasing bone formation, suggesting that α_{1B}-adrenoceptor signalling in osteoblasts plays an important role in bone remodelling under normal conditions. Mice with low activity in the sympathetic nervous system, such as leptin receptor-deficient mice and dopamine ß-hydroxylase-deficient mice, both have a high bone mass due to increased bone formation and decreased bone resorption (Takeda *et al.*, 2002; Elefteriou *et al.*, 2005). Regardless of ß$_2$-adrenoceptor signalling being a key element in the regulation of bone remodelling, female mice with chronic sympathetic hyperactivity due to the double knockout of α_{2A}- and α_{2C}-adrenoceptors, which are presynaptic autoreceptors that negatively regulate noradrenaline release, displayed a high bone mass with increased bone formation and decreased bone resorption (Fonseca *et al.*, 2011). In contrast, the role of α_1-ARs signalling in bone remodelling had not yet been examined in detail. In the present study, we found that the systemic administration of prazosin decreased bone formation and resorption (Figure 2). Consistent with a previous study (Suga *et al.*, 2010), the RANKL-treated RAW264.7 cells contained mRNA encoding α_{1A}-, but not α_{1B}- or α_{1D}-adrenoceptors (data not shown). These indicated that α_{1A}-adrenoceptor signalling in osteoclasts might participate in the reduced bone resorption induced by the blockade of α_1-adrenoceptor signalling.

Further analyses are needed to clarify whether α_{1A}-adrenoceptor signalling in osteoclasts directly stimulates osteoclastogenesis. In addition, this study showed that the mRNAs of α_{1B}-, but not α_{1A}-adrenoceptor subtype, was expressed in BMSCs and differentiated BMSCs (Supporting Information Fig. S1). Taken together with the expression of α_1-adrenoceptor subtypes, these results prompted us to speculate that α_{1B}-adrenoceptor signalling in osteoblasts controls osteoclastogenesis through some osteoblast-derived factors such as RANKL and osteoprotegerin. Osteoclastogenesis is regulated by RANKL, an osteoclast differentiation factor, and osteoprotegerin, a decoy receptor for RANKL, both of which are expressed by osteoblasts (Simonet *et al.,* 1997). However, the results of the genetic experiments revealed that α_{1B}-adrenoceptor-deficient mice had a lower bone mass due to decreased bone formation without affecting bone resorption (Figure 4). These results obtained in mice with global deletion of α_{1B}-adrenoceptors suggest that impaired bone formation was due, at least in part, to a cellular dysfunction in osteoblasts lacking α_{1B}-adrenoceptor signalling and that α_{1B}-adrenoceptor signalling functions in osteoblasts. These mice, however, have confounding systemic effects arising from other cell types and/or tissues. The identity of the cell type in which the sympathetic nervous system acts to regulate bone mass remains to be elucidated in future studies using mice with osteoblast-specific α_{1B}-adrenoceptor ablation. To identify the localization of α_1-adrenoceptor subtypes in bone may be explained by the fact that α_1-adrenoceptor signalling in osteoblast plays an important role on bone formation. Because it was not technically feasible, we did not find any evidence of mRNA or protein of α_1-adrenoceptor subtypes located in bone. Therefore, the definitive role of α_{1B}- adrenoceptors expressed in osteoblasts in the low bone mass observed in this study is still to be confirmed. Thus, these results indicate that the regulation of bone remodelling by the sympathetic nervous system is extremely complex. However, this study showed that not only ß$_2$- but also α_{1B}-adrenoceptor signalling in osteoblasts plays an important role in mediating bone remodelling through the sympathetic nervous system.

The physiological action of adrenaline (epinephrine) was previously demonstrated to be mediated by α_1- as well as ß- adrenoceptor signalling in osteoblasts. Our previous studies also showed that cellular proliferation was facilitated via α_{1B}- adrenoceptors and inhibited via ß- adrenoceptors in human osteoblastic SaM-1 cells (Kodama & Togari, 2013). In the present study, phenylephrine stimulated chloroethylclonidine, cellular proliferation on BMSCs (Supporting Information Fig. S2). In addition, pretreatment with an α_{1B}-adrenoceptor-selective antagonist inhibited phenylephrine-induced *Cebpd* expression in MC3T3-E1 osteoblastic cells (data not shown). Furthermore, we observed that phenylephrine-induced cellular proliferation was significantly decreased in MC3T3-E1 cells transfected with *Cebpd* siRNA. Based on these results and our previous findings, we suggested that α_{1B}- adrenoceptor signalling mediated cellular proliferation through a mechanism relevant to the up-regulation of Cebpd in osteoblasts, and that the α_1- adrenoceptor signalling by osteoblasts might participate in the mechanism underlying the regulation of bone formation by the sympathetic nervous system.

In conclusion, our results suggest that α_{1B}- adrenoceptor signalling in osteoblasts is required for bone formation and regulates cellular proliferation through the up-regulation of Cebpd and, thus, provide new evidence for the physiological importance of α_{1B}- adrenoceptor signalling in bone homeostasis. In humans, a series of studies showed that an α-blocker was associated with an increased risk of hip/femur fracture (Souverein *et al.,* 2003; Song *et al.,* 2012). A clearer understanding of the functions of the α_{1B}- adrenoceptor and its interactions with ß$_2$- adrenoceptors in bone remodelling will assist in elucidating the role of the sympathetic nervous system in bone metabolism, which will, in turn, facilitate the development of novel therapeutic strategies for the treatment of osteoporosis.

Acknowledgements

This work was supported in part by Grants-in-Aid for Scientific Research to D. K. (24791988), H. K. (15 K11061), and to A. T. (26462827) from the Ministry of Education, Culture, Sports, Science and Technology, Japan. We thank Dr Akito Tanoue of the Department of Pharmacology, National Research Institute for Child Health and Development for providing us with α_{1B}-AR-deficient mice.

Author contributions

K. T., T. H., D. K., H. K., K. H. and A. T. designed the research study. K. T. and T. H. performed the experiments and analysed the data. T. H. wrote the paper.

Conflict of interest

The authors declare no conflicts of interest.

Declaration of transparency and scientific rigour

This Declaration acknowledges that this paper adheres to the principles for transparent reporting and scientific rigour of preclinical research recommended by funding agencies, publishers and other organisations engaged with supporting research.

References

Alexander SPH, Davenport AP, Kelly E, Marrion N, Peters JA, Benson HE, *et al.* (2015a). The Concise Guide to PHARMACOLOGY 2015/16: G protein-coupled receptors. Br J Pharmacol 172: 5744–5869.

Alexander SPH, Fabbro D, Kelly E, Marrion N, Peters JA, Benson HE, *et al.* (2015b). The Concise Guide to PHARMACOLOGY 2015/16: Catalytic receptors. Br J Pharmacol 172: 5979–6023.

Alexander SPH, Fabbro D, Kelly E, Marrion N, Peters JA, Benson HE, *et al.* (2015c). The Concise Guide to PHARMACOLOGY 2015/16: Enzymes. Br J Pharmacol 172: 6024–6109.

Balamurugan K, Sterneck E (2013). The many faces of C/EBPdelta and their relevance for inflammation and cancer. Int J Biol Sci 9: 917–933.

Barbaro V, Testa A, Di Iorio E, Mavilio F, Pellegrini G, De Luca M (2007). C/EBP delta regulates cell cycle and self-renewal of human limbal stem cells. J Cell Biol 177: 1037–1049.

Cavalli A, Lattion AL, Hummler E, Nenniger M, Pedrazzini T, Aubert JF, *et al.* (1997). Decreased blood pressure response in mice deficient of the alpha1b-adrenergic receptor. Proc Natl Acad Sci USA 94: 11 589–11 594.

Curtis MJ, Bond RA, Spina D, Ahluwalia A, Alexander SPA, Giembycz MA, *et al.* (2015). Experimental design and analysis and their reporting: new guidance for publication in BJP. Br J Pharmacol 172: 3461–3471.

Elefteriou F, Ahn JD, Takeda S, Starbuck M, Yang X, Liu X, *et al.* (2005). Leptin regulation of bone resorption by the sympathetic nervous system and CART. Nature 434: 514–520.

Fonseca TL, Jorgetti V, Costa CC, Capelo LP, Covarrubias AE, Moulatlet AC, *et al.* (2011). Double disruption of α2A- and α2C-adrenoceptors results in sympathetic hyperactivity and high-bone-mass phenotype. J Bone Miner Res 26: 591–603.

Gery S, Tanosaki S, Hofmann WK, Koppel A, Koeffler HP (2005). C/EBP delta expression in a BCR-ABL-positive cell line induces growth arrest and myeloid differentiation. Oncogene 24: 1589–1597.

Gutierrez S, Javed A, Tennant DK, van Rees M, Montecino M, Stein GS, *et al.* (2002). CCAAT/enhancer-binding proteins (C/EBP) ß and δ activate osteocalcin gene transcription and synergize with runx2 at the C/EBP element to regulate bone-specific expression. J Biol Chem 277: 1316–1323.

Hanson RW (1998). Biological role of the isoforms of C/EBP minireview series. J Biol Chem 273: 28 543.

Hirai T, Tokumo K, Tsuchiya D, Nishio H (2009). Expression of mRNA for 5-HT_2 receptors and proteins related to inactivation of 5-HT in mouse osteoblasts. J Pharmacol Sci 109: 319–323.

Hirai T, Tanaka K, Togari A (2014a). α1-adrenergic receptor signaling in osteoblasts regulates clock genes and bone morphogenetic protein 4 expression through up-regulation of the transcriptional factor nuclear factor IL-3 (Nfil3)/E4 promoter-binding protein 4 (E4BP4). J Biol Chem 289: 17 174–17 183.

Hirai T, Tanaka K, Togari A (2014b). ß-adrenergic receptor signaling regulates *Ptgs2* by driving circadian gene expression in osteoblasts. J Cell Sci 127: 3711–3719.

Hirai T, Tanaka K, Togari A (2015a). α_{1B}-adrenergic receptor signaling controls circadian expression of the *Tnfrsf11b* by regulating clock genes in osteoblasts. Biol Open 4: 1400–1409.

Hirai T, Kobayashi T, Nishimori S, Karaplis AC, Goltzman D, Kronenberg HM (2015b). Bone is a major target of PTH/PTHrP receptor signaling in regulation of fetal blood calcium homeostasis. Endocrinology 156: 2774–2780.

Huang HH, Brennan TC, Muir MM, Mason RS (2009). Functional alpha1- and beta2-adrenergic receptors in human osteoblasts. J Cell Physiol 220: 267–275.

Kilkenny C, Browne W, Cuthill IC, Emerson M, Altman DG (2010). NC3Rs Reporting Guidelines Working Group. Br J Pharmacol 160: 1577–1579.

Kobilka BK (2011). Structural insights into adrenergic receptor function and pharmacology. Trends Pharmacol Sci 32: 213–218.

Kodama D, Togari A (2013). Noradrenaline stimulates cell proliferation by suppressing potassium channels via G(i/o)-protein-coupled α1(1B)-adrenoceptors in human osteoblasts. Br J Pharmacol 168: 1230–1239.

Kondo M, Kondo H, Miyazawa K, Goto S, Togari A (2013). Experimental tooth movement-induced osteoclast activation is regulated by sympathetic signaling. Bone 52: 39–47.

McGrath JC, Lilley E (2015). Implementing guidelines on reporting research using animals (ARRIVE etc.): new requirements for publication in BJP. Br J Pharmacol 172: 3189–3193.

Obata K, Furuno T, Nakanishi M, Togari A (2007). Direct neurite-osteoblastic cell communication, as demonstrated by use of an in vitro co-culture system. FEBS Lett 581: 5917–5922.

O'Rourke JP, Newbound GC, Hutt JA, Dewille J (1999). CCAAT/enhancer-binding protein delta regulates mammary epithelial cell G0 growth arrest and apoptosis. J Biol Chem 274: 16 582–16 589.

Pawson AJ, Sharman JL, Benson HE, Faccenda E, Alexander SP, Buneman OP *et al.*, NC-IUPHAR (2014). The IUPHAR/BPS guide to PHARMACOLOGY: an expert-driven knowledge base of drug targets and their ligands. Nucleic Acids Res 42: D1098–D1106.

Ramji DP, Foka P (2002). CCAAT/enhancer-binding proteins: structure, function and regulation. Biochem J 365: 561–575.

Sarkar TR, Sharan S, Wang J, Pawar SA, Cantwell CA, Johnson PF, *et al.* (2012). Identification of a Src tyrosine kinase/SIAH2 E3 ubiquitin ligase pathway that regulates C/EBP delta expression and contributes to transformation of breast tumor cells. Mol Cell Biol 32: 320–332.

Simonet WS, Lacey DL, Dunstan CR, Kelley M, Chang MS, Lüthy R, *et al.* (1997). Osteoprotegerin: a novel secreted protein involved in the regulation of bone density. Cell 89: 309–319.

Song HJ, Lee J, Kim YJ, Jung SY, Kim HJ, Choi NK, *et al.* (2012). ß1 selectivity of ß-blockers and reduced risk of fractures in elderly hypertension patients. Bone 51: 1008–1015.

Souverein PC, Van Staa TP, Egberts AC, De la Rosette JJ, Cooper C, Leufkens HG (2003). Use of alpha-blockers and the risk of hip/femur fractures. J Intern Med 254: 548–554.

Suga S, Goto S, Togari A (2010). Demonstration of direct neurite-osteoclastic cell communication *in vitro* via the adrenergic receptor. J Pharmacol Sci 112: 184–191.

Suzuki A, Palmer G, Bonjour JP, Caverzasio J (1998). Catecholamines stimulate the proliferation and alkaline phosphatase activity of MC3T3-E1 osteoblast-like cells. Bone 23: 197–203.

Suzuki A, Palmer G, Bonjour JP, Caverzasio J (1999). Regulation of alkaline phosphatase activity by p38 MAP kinase in response to activation of Gi protein-coupled receptors by epinephrine in osteoblast-like cells. Endocrinology 140: 3177–3182.

Takeda S, Elefteriou F, Levasseur R, Liu X, Zhao L, Parker KL, *et al.* (2002). Leptin regulates bone formation via the sympathetic nervous system. Cell 111: 305–317.

Takeuchi T, Tsuboi T, Arai M, Togari A (2001). Adrenergic stimulation of osteoclastogenesis mediated by expression of osteoclast differentiation factor in MC3T3-E1 osteoblast-like cells. Biochem Pharmacol 61: 579–586.

Tanaka K, Hirai T, Ishibashi Y, Izumo N, Togari A (2015). Modulation of osteoblast differentiation and bone mass by 5-HT_{2A} receptor signaling in mice. Eur J Pharmacol 762: 150–157.

Thangaraju M, Rudelius M, Bierie B, Raffeld M, Sharan S, Hennighausen L, *et al.* (2005). C/EBP delta is a crucial regulator of pro-apoptotic gene expression during mammary gland involution. Development 132: 4675–4685.

Togari A, Arai M, Kondo A (2005). The role of the sympathetic nervous system in controlling bone metabolism. Expert Opin Ther Targets 9: 931–940.

Togari A (2002). Adrenergic regulation of bone metabolism: possible involvement of sympathetic innervation of osteoblastic and osteoclastic cells. Microsc Res Tech 58: 77–84.

Umayahara Y, Billiard J, Ji C, Centrella M, McCarthy TL, Rotwein P (1999). CCAAT/enhancer-binding protein delta is a critical regulator

of insulin-like growth factor-I gene transcription in osteoblasts. J Biol Chem 274: 10 609–10 617.

Yamanaka R, Lekstrom-Himes J, Barlow C, Wynshaw-Boris A, Xanthopoulos KG (1998). CCAAT/enhancer binding proteins are critical components of the transcriptional regulation of hematopoiesis. Int J Mol Med 1: 213–221.

Supporting Information

Additional Supporting Information may be found in the online version of this article at the publisher's web-site:

http://dx.doi.org/10.1111/bph.13418

Figure S1 Gene expression of α1-AR subtypes in bone cells. In order to determine the α1-AR subtypes expressed by osteoblasts, we performed real-time PCR using primers specific for each receptor subtype in BMSCs and MC3T3-E1 cells. Relative mRNA expression was normalized to Gapdh. Figures are representative of data from six independent determinations. α1A-AR, α1B-AR, and α1D-AR transcripts were detected in C3H10T1/2 cells as a positive control. ND, not detected.

Figure S2 PHE stimulated cellular proliferation in BMSCs. Cells were treated with PHE at 0.03 to 0.3 μM for 24 h, followed by the determination of BrdU incorporation (mean ± SEM). Each value represents the means ± SEM of six independent determinations. *, $P < 0.05$, significantly different from control value.